Dyes and Pigments 81 (2009) 10–17

Contents lists available at ScienceDirect

Dyes and Pigments

journal homepage: www.elsevier.com/locate/dyepig

The synthesis, two-photon absorption and blue upconversion fluorescence of novel, nitrogen-containing heterocyclic chromophores

Yi-Feng Sun [a,b], Wei Huang [a], Chang-Gui Lu [a], Yi-Ping Cui [a,*]

[a] Advanced Photonics Center, School of Electronic Science and Engineering, Southeast University, Nanjing 210096, China
[b] Department of Chemistry, Taishan University, Taian 271021, China

ARTICLE INFO

Article history:
Received 10 July 2008
Received in revised form 3 August 2008
Accepted 6 August 2008
Available online 22 August 2008

Keywords:
Two-photon absorption
Nonlinear transmission
Heterocycle
1,2,4-Triazine
Imidazole
Crystal structure

ABSTRACT

Novel, nitrogen-containing heterocyclic chromophores based on either 1,2,4-triazine or an imidazole core were synthesized using a three-component, one-pot reaction under microwave irradiation. Structures were verified by ^{1}H NMR, IR, MS and elemental analyses while crystal structure was determined using X-ray diffraction. The two-photon absorption and two-photon upconverted blue fluorescent emission characteristics were investigated experimentally; preliminary structure–photophysical property relationships were established. Chromophores that contained the imidazole moiety displayed more potent two-photon absorption than compounds based upon 1,2,4-triazine and also exhibited a strong two-photon upconverted blue fluorescent emission peak at around 443–476 nm. Significant enhancement of the two-photon absorption cross-section was achieved by fusing a benzoxazole moiety onto the phenanthro[9,10-*d*]imidazole ring.

1. Introduction

A tremendous amount of recent attention has been attracted to synthesize and investigate the behaviors of organic molecules with two-photon absorption (TPA) properties for their potential applications in materials science and biological imaging [1–5]. Efficient TPA molecules with different emission wavelengths for biological imaging applications are helpful to reduce background light scattering and auto-fluorescence from fluorescence proteins in biological cells and organisms. For example, efficient two-photon induced blue emitting molecules could be used to reduce the auto-fluorescence background from green and red proteins [6]. Obviously, the development of new molecules with large TPA cross-sections and efficient upconverted fluorescence at desirable wavelengths is of fundamental importance in advancing techniques for laser spectroscopy, laser processing and non-invasive monitoring of diseased tissues. Although large numbers of TPA organic molecules have been reported to date [7–10], the emitting wavelengths of these molecules locate mostly in the 500–700 nm region, and there is still an intense demand for TPA molecules with efficient blue emission in both basic and applied science. Therefore, an investigation of the synthesis and properties of TPA molecules with efficient two-photon induced blue emission has been and remains an urgent and interesting area of research.

Among these reported TPA systems, the heterocycle-based chromophores represent an emerging and growing class of TPA materials, and have evoked much attention [11–14]. This is connected with their intrinsic chemically tunable molecular structures and easily delocalizable heteroaromatic rings which can help to improve their degree of intramolecular charge transfer (ICT) [15].

Nitrogen heterocycles are of special interest because they constitute an important class of natural and nonnatural products, many of which exhibit useful biological activities and unique electrical and optical properties [16–20]. Furthermore, the concern with five-membered heterocyclic imidazole or oxazole derivatives has been growing because these compounds have a number of optical applications, such as fluorescence compounds, dyes, and TPA materials [21–24]. Also, many commercial fluorescent brighteners for application to synthetic fibers contain an imidazole or oxazole moiety [25], and both imidazoles are easy to synthesize and oxazoles are readily available.

On the other hand, as an important kind of organic six-membered heterocycles, 1,2,4-triazine derivatives have been used as ligands for complexation of metal ions and as extracting agents for partitioning of minor actinides [26]. In particular, some of them are also found to be efficient fluorescent chemosensors for recognition of transition metal ions such as Cu^{2+} [27]. To the best of our knowledge, however, unlike the 1,3,5-*s*-triazines, this kind of molecule based on 1,2,4-triazine acceptor has never been studied as a TPA material.

In view of the possible importance of these heterocycle-based chromophores and the continued interest in the development of

* Corresponding author. Tel.: +86 25 83792470; fax: +86 25 83601769.
E-mail address: cyp@seu.edu.cn (Y.-P. Cui).

0143-7208/$ – see front matter © 2008 Elsevier Ltd. All rights reserved.
doi:10.1016/j.dyepig.2008.08.003

TPA materials, in the present work, we wish to report on the syntheses of six new TPA chromophores based on the 1,2,4-triazine or imidazole core, including two 1,2,4-triazine derivatives (**DS1** and **DS2**) and four imidazole derivatives (**DS3**–**DS6**), under microwave irradiation. Specially, we have focused on the coupling of two readily available substrates, imidazole and benzoxazole. Our purpose is that it would be more likely to obtain organic molecules with TPA properties from these excellent molecular moieties. Consequently, two imidazole–oxazole hybrids (**DS3** and **DS4**) have been synthesized. It is expected that the fusion of an oxazole moiety to the imidazole ring system may result in an enhanced molecular TPA properties of compounds. At the same time, the TPA properties of five heterocycle-based chromophores (**DS1**–**DS5**) were investigated by nonlinear transmission method with femtosecond laser pulses in solution. Additionally, in order to investigate the real three-dimensional structure of imidazole-based chromophores, the crystal of **DS6** was obtained, and the structure was determined by X-ray diffraction technique. The synthetic pathway and the structures of target molecules are shown in Fig. 1.

2. Experimental

2.1. Chemicals and instrument

All melting points were determined with a WRS-1A melting point apparatus and are uncorrected. Proton nuclear magnetic resonance (^{1}H NMR) spectra were run on a Bruker AV-400 NMR spectrometer and chemical shifts expressed as δ (ppm) values with TMS as internal standard. IR spectra were recorded in KBr on a Nicolet NEXUS 470 FT-IR spectrophotometer. Vibrational transition frequencies are reported in wave numbers (cm^{-1}). Element analysis was taken with a Perkin–Elmer 240 analyzer. Mass spectra (MS) were measured on a VG ZAB-HS mass spectrometer. Single crystal was characterized by Bruker Smart 1000 CCD X-ray single crystal diffractometer. All the chemicals are commercially available and they were used without further purification. All solvents were dried using standard methods before use.

2.2. Synthesis

2.2.1. Preparation of bis-1,2,4-triazine derivatives *DS1*, *DS2*

Two bis-1,2,4-triazine derivatives were synthesized from benzil, dihydrazide and ammonium acetate in the glacial acetic acid under microwave irradiation according to the method reported by us previously [27].

*2.2.1.1. 1,4-Bis(5,6-diphenyl-1,2,4-triazin-3-yl)benzene (**DS1**).* Yield 57%; mp 309–312 °C. ^{1}H NMR ($CDCl_3$/TMS) δ: 7.41–7.53 (m, 12H), 7.68 (d, $J = 7.3$ Hz, 4H), 7.74 (d, $J = 7.8$ Hz, 4H), 8.90 (s, 4H). IR (KBr) ν: 3058, 1674, 1598, 1578, 1504, 1491, 1444, 1386, 1356, 1271, 1128, 1081, 1016, 868, 821, 767, 760, 694, 591, 528 cm^{-1}. FAB-MS m/z: 541 (M + 1). Anal. calcd for $C_{36}H_{24}N_6$: C 79.98, H 4.47, N 15.54; found: C 80.12, H 4.56, N 15.38.

*2.2.1.2. 1,3-Bis(5,6-diphenyl-1,2,4-triazin-3-yl)benzene (**DS2**).* Yield 63%; mp 298–300 °C. ^{1}H NMR ($CDCl_3$/TMS) δ: 7.40–7.54 (m, 13H), 7.68 (d, $J = 7.3$ Hz, 4H), 7.78 (d, $J = 7.8$ Hz, 4H), 8.93 (dd, $J_1 = 7.8$, $J_2 = 1.6$, 2H), 9.96 (s, 1H). IR (KBr) ν: 3052, 1598, 1579, 1504, 1491, 1435, 1379, 1372, 1241, 1171, 1076, 1003, 994, 923, 807, 769, 758, 704, 693, 591, 534, 508 cm^{-1}. FAB-MS m/z: 541 (M + 1). Anal. calcd for $C_{36}H_{24}N_6$: C 79.98, H 4.47, N 15.54; found: C 79.84, H 4.41, N 15.45.

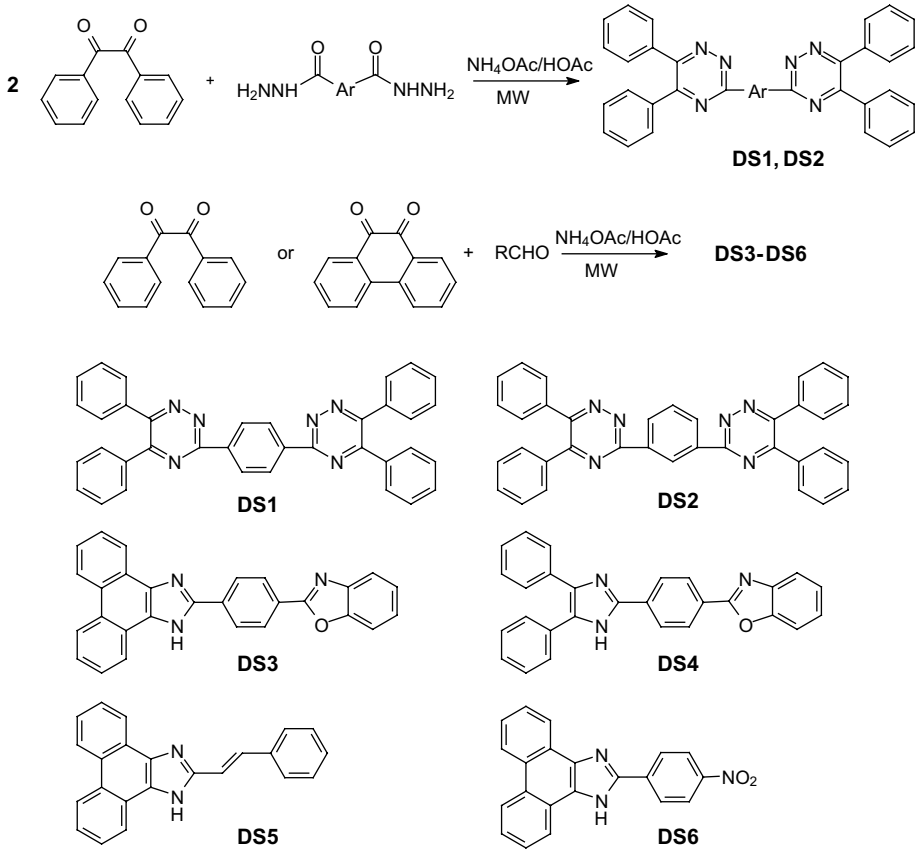

Fig. 1. The synthetic pathway and the structures of target molecules.

*2.2.2. General procedure for the synthesis of imidazole derivatives **DS3–DS6***

For the preparation of compounds **DS3–DS6**, 2 mmol of 9,10-phenanthraquinone or benzil, 2 mmol of appropriate aryl aldehydes, 12 mmol of ammonium acetate and 20 mL of glacial acetic acid were mixed together at ambient temperature. The mixture was irradiated in a Galanz microwave oven for an optimized time and taken out for a few seconds and at the same time, the mixture was stirred carefully using a bar. The mixture was subjected to microwave irradiation for another optimized time and then taken out for stirring. The operation was repeated several times, and the reaction mixture was monitored by TLC. After the reaction was completed, the reaction mixture was poured into ice–water. The solid product was collected on a filter, and then washed thoroughly with cold water, dried and recrystallized from EtOH–DMF.

*2.2.2.1. 2-(4-(1*H*-phenanthro[9,10-*d*]imidazol-2-yl)phenyl) benzoxazole (**DS3**).* Yield 72%; mp 307–309 °C. ^{1}H NMR (DMSO-d_6/TMS) δ: 7.44–7.87 (m, 8H), 8.43 (d, $J = 8.6$ Hz, 2H), 8.55 (d, $J = 8.4$ Hz, 2H), 8.57–8.90 (m, 4H), 13.66 (s, 1H). IR (KBr) ν: 3436, 3049, 1662, 1615, 1571, 1564, 1519, 1482, 1454, 1430, 1350, 1289, 1245, 1184, 1109, 1057, 1012, 958, 928, 892, 851, 813, 762, 745, 725, 711, 684, 511, 436 cm^{-1}. FAB-MS *m*/*z*: 412 (M + 1). Anal. calcd for $C_{28}H_{17}N_3O$: C 81.73, H 4.16, N 10.21; found: C 81.62, H 4.35, N 10.07.

*2.2.2.2. 2-(4-(4,5-Diphenyl-1*H*-imidazol-2-yl)phenyl) benzoxazole (**DS4**).* Yield 69%; mp 301–302 °C. ^{1}H NMR (DMSO-d_6/TMS) δ: 7.30–8.43 (m, 18H). 13.42 (s, 1H). IR (KBr) ν: 3420, 3035, 1616, 1602, 1585, 1530, 1504, 1488, 1450, 1442, 1435, 1388, 1344, 1288, 1243, 1181, 1126, 1055, 968, 849, 810, 764, 740, 696, 510 cm^{-1}. FAB-MS *m*/*z*: 414 (M + 1). Anal. calcd for $C_{28}H_{19}N_3O$: C 81.34, H 4.63, N 10.16; found: C 81.23, H 4.47, N 10.06.

*2.2.2.3. 2-Styryl-1*H*-phenanthro[9,10-*d*]imidazole (**DS5**).* Yield 58%; mp 172–174 °C. ^{1}H NMR (DMSO-d_6/TMS) δ: 7.35–7.78 (m, 11H), 8.49 (d, $J = 8.2$ Hz, 2H), 8.85 (d, $J = 7.6$ Hz, 2H), 13.36 (s, 1H). IR (KBr) ν: 3423, 3054, 1655, 1614, 1581, 1571, 1504, 1449, 1413, 1384, 1342, 1236, 1070, 1018, 964, 852, 744, 720, 681, 540, 497, 434 cm^{-1}. FAB-MS *m*/*z*: 321 (M + 1). Anal. calcd for $C_{23}H_{16}N_2$: C 86.22, H 5.03, N 8.74; found: C 86.31, H 4.95, N 8.94.

*2.2.2.4. 2-(4-Nitrophenyl)-1*H*-phenanthro[9,10-*d*]imidazole (**DS6**).* Yield 62%; mp >300 °C. ^{1}H NMR (DMSO-d_6) δ: 7.66–7.78(m, 4H), 8.46(d, $J = 7.8$ Hz, 2H), 8.54–8.60 (m, 4H), 8.87 (d, $J = 7.2$ Hz, 2H), 13.82 (s, 1H). FAB-MS: 340 (M + 1).

2.3. Photophysical methods

The linear absorption spectra were recorded on a Shimadzu UV-3600PC scanning spectrophotometer with 1 nm resolution. The one-photon fluorescence spectra were measured by a Perkin–Elmer LS50B fluorescence spectrophotometer in a 1-cm path length cell.

TPA cross-section (σ_2) values were determined using nonlinear transmission (NLT) method [7,28] with femtosecond laser pulses. In measurement of nonlinear transmission, the excitation source is a Ti:sapphire oscillator system/amplifier (Mira900-F, Legend-F from Coherent Inc.) producing ~300 fs duration, 800 nm wavelength laser output with a repetition rate of 1 kHz. The incident laser pulses were focused *via* an $f = 15$ cm lens onto the center of the sample cell which is a 1 cm-length quartz cuvette. Samples were dissolved in chloroform or DMF with a concentration value of 1×10^{-2} M. Pure solvent was used as reference to eliminate the attenuation influences from the cell windows and the solvent itself to transmitted intensity. The TPA coefficient β of the sample solution could be determined by Eq. (1). Furthermore, the TPA cross-section σ_2 (in unit of cm^4 s/photon or GM, 1 GM = 10^{-50} s/photon) of the sample was calculated by Eq. (2) [7].

$$T = I(L)/I_0 = [\ln(l + I_0 L\beta)]/I_0 L\beta \quad (1)$$

$$\beta = \sigma_2 N_0/h\nu = \sigma_2 N_A d \times 10^{-3}/h\nu \quad (2)$$

Here, T is the transmissivity of the sample solution, I_0 is the incident intensity, $I(L)$ is the transmitted intensity, L is the thickness of the sample cell, $h\nu$ is the energy of an incident photon, N_0 is the molecular density of sample, N_A is the Avogadro constant, d is the concentration of the sample solution.

Two-photon fluorescence spectra are obtained by using 0.300 Meter Triple Grating monochrometor/spectrograph from Acton Research Corporation.

2.4. X-ray crystallography

Suitable single crystal of **DS6** for X-ray structural analysis was obtained by evaporation of DMF solution. The diffraction data were collected with a Bruker Smart Apex 1000 CCD area detector using a graphite monochromated Mo Kα radiation ($\lambda = 0.71073$ Å) at 273(2) K. The structure was solved by direct methods with SHELXS-97 program and refinements on F^2 were performed with SHELXL-97 program by full-matrix least-squares techniques with anisotropic thermal parameters for the non-hydrogen atoms. All hydrogen atoms were added according to a theoretical model. A summary of the crystallographic data and structure refinement details is given in Table 1.

3. Results and discussion

3.1. Synthesis

Two bis-1,2,4-triazine derivatives **DS1** and **DS2** were prepared from benzil, 1,4(or 1,3)-benzenedicarbohydrazide, and ammonium

Table 1
Crystal data and structure refinement for **DS6**

Empirical formula	$C_{21}H_{13}N_3O_2 \cdot C_3H_7NO$
Formula weight	412.44
Temperature (K)	273(2)
Crystal system	Triclinic
Space group	$P\bar{1}$
Unit cell dimensions	
a (Å)	8.662(2)
b (Å)	10.607(3)
c (Å)	11.829(3)
α (°)	93.980(19)
β (°)	103.126(17)
γ (°)	102.237(18)
Volume (Å^3), Z	1026.5(4), 2
D_{calc} (Mg/m^3)	1.334
Absorption coefficient (mm^{-1})	0.090
F (000)	432
Crystal size (mm)	0.15 × 0.12 × 0.10
θ Range for data collection (°)	1.78–25.05
Limiting indices	$-10 \le h \le 10$
	$-12 \le k \le 12$
	$-14 \le l \le 13$
Reflections collected/unique	7866/3642
	[$R_{int} = 0.0224$]
Max. and min. transmission	0.9910 and 0.9866
Data/restraints/parameters	3642/0/283
Goodness-of-fit on F^2	1.057
Final R indices [$I > 2$sigma(I)]	$R_1 = 0.0489$
	$wR_2 = 0.1299$
R indices (all data)	$R_1 = 0.0719$
	$wR_2 = 0.1455$
Extinction coefficient	0.008(2)
Largest diff. peak and hole (e Å^{-3})	0.270 and −0.201
CCDC	680351

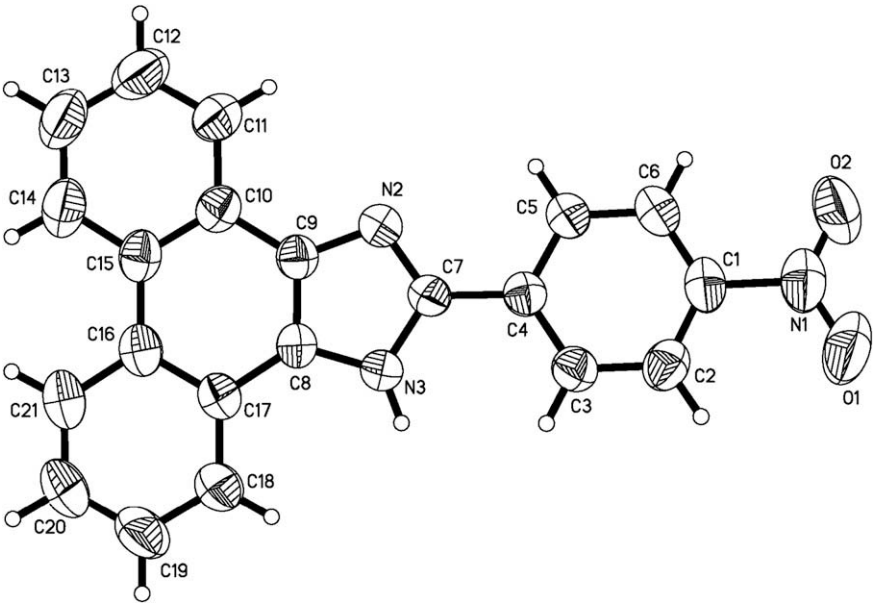

Fig. 2. The molecular structure of **DS6**, showing the atom-labelling scheme. Displacement ellipsoids are drawn at the 50% probability level. H atoms are shown as small spheres of arbitrary radius. DMF molecule is omitted for clarity.

acetate in glacial acetic acid under microwave irradiation according to the method reported by us previously as shown in Fig. 1 [27]. A similar treatment yields substituted imidazoles **DS3**–**DS6** by the one-pot condensation of 9,10-phenanthraquinone or benzil, appropriate aryl aldehydes, in glacial acetic acid using ammonium acetate as the ammonia source under microwave irradiation (Fig. 1). It is noteworthy that the reactions which required 2–5 h in conventional method, was completed efficiently, with 57–72% yields, in 5–12 min under microwave conditions and the products were easily collected and purified in these two experiments. Therefore, such a microwave procedure could offer a simple method for synthesizing various 1,2,4-triazines and imidazoles *via* three-component, one-pot reaction of dihydrazide or aldehydes with symmetrical 1,2-diketones and ammonium acetate.

All the synthesized compounds have been characterized on the basis of their physical data and spectral analysis. The IR spectra of compounds **DS3**–**DS6** exhibit absorption frequency at 3420–3436 cm^{-1} for NH group of imidazole. All the compounds show the NMR signals for different kinds of protons at their respective positions. The values are consistent with their predicted structures (Fig. 1).

3.2. Crystal structure

It was reported that most of the imidazole derivatives form inclusion compounds with various guest molecules [21]. Also, the crystal structure of these compounds showed that solvent of crystallization and intermolecular hydrogen bonds play an essential role in the chromotropic behavior and in the packing of molecules in the crystals.

Although compound **DS6** has been studied previously by other groups [29], the crystal structure of **DS6** has not been reported. A structure analysis reveals that the present compound, **DS6**, formed crystalline clathrates with DMF in a 1:1 molar ratio. The crystal structure of **DS6** is shown in Fig. 2. As can be seen from Fig. 2, the imidazole ring (N2/N3/C7–C9) and phenanthrene ring system (C8–C21) are almost coplanar [r.m.s. deviation = 0.0344 Å, maximum deviation = −0.0561(2) Å for atom C19], which suggests the phenanthro[9,10-*d*]imidazole moiety deviates only slightly from being fully planar. On the other hand, the benzene ring (C1–C6) is slightly twisted out of the plane of the phenanthro[9,10-*d*]imidazole ring system (N2/N3/C7–C21) by 11.3°, which indicates that the whole molecule is nearly planar (Fig. 3). Comparison with 2-phenylimidazo[4,5-*f*] phenanthroline [30] suggests that the presence of 4-NO_2 group leads to this deviation from coplanarity. This is in marked contrast to the orientations in 2,4,5-triphenyl imidazole derivatives [24,31], in which the planes of the three phenyl rings all twist out of the imidazole plane.

In addition, the bond length, 1.460(3) Å, is that of the C4–C7 bond linking the benzene and imidazole rings and is, as expected, shorter than a normal C–C single bond (1.54 Å). Therefore, it could be suggested that the benzene ring is highly conjugated with the phenanthro[9,10-*d*]imidazole ring system.

Similar geometry has been observed in 2-(4-hydroxy-3,5-dimethoxyphenyl)-1*H*-phenanthro[9,10-*d*]imidazole [32], which were reported by us previously. In 2-(4-hydroxy-3,5-dimethoxyphenyl)-1*H*-phenanthro[9,10-*d*]imidazole, though the phenanthrene ring is slightly bent, and a dihedral angle of 4.7° is found between the mean planes of the imidazole ring (N1/N2/C9–C11) and phenanthrene ring system (C10–C23), which is larger than that of 3.3° in DS6, these two ring systems are approximately coplanar [r.m.s. deviation = 0.0607 Å, maximum deviation = 0.1408(2) Å for atom N1].

Therefore, the 2-phenylphenanthro[9,10-*d*]imidazole moiety possess a larger conjugated system and highly molecular planarity. These structural features based on the X-ray crystallographic

Fig. 3. The side elevation of **DS6**. DMF molecule and H atoms are omitted for clarity.

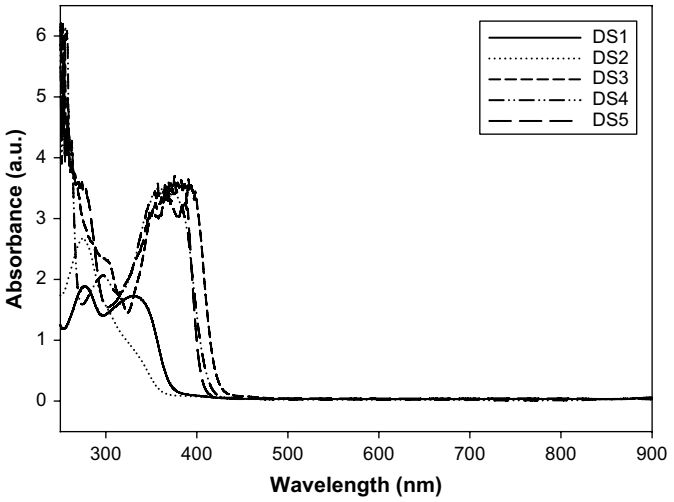

Fig. 4. The linear absorption spectra of the chromophores **DS1**–**DS5**.

analysis lead us to believe that this kind of conjugated framework containing 2-phenylphenanthro[9,10-*d*]imidazole moiety could be a useful conjugated building block with potential applications in forming new kind of effective organic two-photon induced fluorescence (TPIF) molecules.

3.3. Linear photophysical properties

According to their molecular structure, the compounds investigated here could be classed into two types, bis-1,2,4-triazines (**DS1** and **DS2**) and imidazoles (**DS3**–**DS5**) (Fig. 1). As seen from Fig. 1, for two bis-1,2,4-triazine derivatives **DS1** and **DS2**, structural modification occurs only in one central unit, where a 1,4-phenylene was replaced by a 1,3-phenylene. Such a modification could be expected to result in some changes in the π-conjugated length and in the absorption and emission spectra. On the other hand, three compounds **DS3**–**DS5** contain an imidazole core. These molecules are related, but their chemical structures are differentiated by introducing various moieties, for instance phenyl, phenanthryl, 4-benzoxazol-2-ylphenyl, or styryl, in order to provide a means for studying structure–property relationships.

The linear absorption spectra of **DS1**, **DS2** in chloroform (3×10^{-6} mol L^{-1}) and **DS3**–**DS5** in DMF (1×10^{-5} mol L^{-1}) solutions are presented in Fig. 4. There is no reasonable linear

Table 2
One- and two-photon properties of the chromophores **DS1**–**DS5**

Compounds	$\lambda^{abs}{}_{max}$[a] (nm)	$\lambda^{spf}{}_{max}$[a] (nm)	$\triangle\nu$[b] (cm^{-1})	$\lambda^{tpf}{}_{max}$[a] (nm)	β[c](cm/GW)	σ_2 (GM)[d]
DS1	276	483	15,528	–[e]	0.0016	6.608
DS2	275	460	14,624	–[e]	0.0011	4.543
DS3	376	461	4904	476	0.0050	20.650
DS4	357	463	6413	474	0.0038	15.694
DS5	367	434	4206	443	0.0018	7.434

[a] $\lambda^{abs}{}_{max}$, $\lambda^{spf}{}_{max}$, $\lambda^{tpf}{}_{max}$: peak wavelengths in the linear absorption, one-photon excited fluorescence and two-photon excited fluorescence spectra.
[b] Stokes shift in $cm^{-1}(1/\lambda^{abs}{}_{max}-1/\lambda^{spf}{}_{max})$.
[c] TPA coefficient.
[d] TPA cross-section values given in GM at 800 nm, 1 GM = 1×10^{-50} cm^4 s per photon per molecule.
[e] Weak fluorescence cannot be detected.

absorption for all compounds in the entire spectral range above 450 nm. As shown in Fig. 4, the absorption spectrum of **DS1** shows two sharp absorptions at $\lambda_{max}=276$ and 331 nm, respectively. Compared with **DS1**, an important feature of the absorption spectra of **DS2** is that an absorption peak was observed at 275 nm with weak shoulder peak at the longer wavelength side, which suggested that the conjugation of 1,4-phenylene in **DS1** is larger than that of 1,3-phenylene skeleton in **DS2**.

Let us now turn our attention towards the compounds of imidazoles, **DS3**–**DS5**. Although these three compounds have very similar absorption spectra, and present a strong intramolecular charge transfer (ICT) absorption band within 320–430 nm, the maximum absorption peaks of ICT absorption band undergo a red-shift from **DS4** (357 nm) to **DS5** (367 nm), and to **DS3** (376 nm).

Concerning compounds **DS3** and **DS4**, the phenanthro[9,10-*d*]imidazole system for **DS3** caused a bathochromic effect of approximately 19 nm relative to the diphenyl imidazole system for **DS4**, suggesting that the conjugation of phenanthro[9,10-*d*]imidazole system is larger than that of diphenyl imidazole system. As a result, the red-shift of absorption can possibly occur. It was also noted that replacement of 4-benzoxazol-2-yl phenyl group with a styryl donor in one terminal moiety of the phenanthro[9,10-*d*]imidazole molecules resulted in a slight hypsochromic shift (9 nm), which implied that **DS3** seems to possess a larger conjugated system than **DS5**.

Actually, based on the X-ray structure analysis findings, it could be found that the 2-phenylphenanthro[9,10-*d*]imidazole moiety possess a larger conjugated system and highly molecular

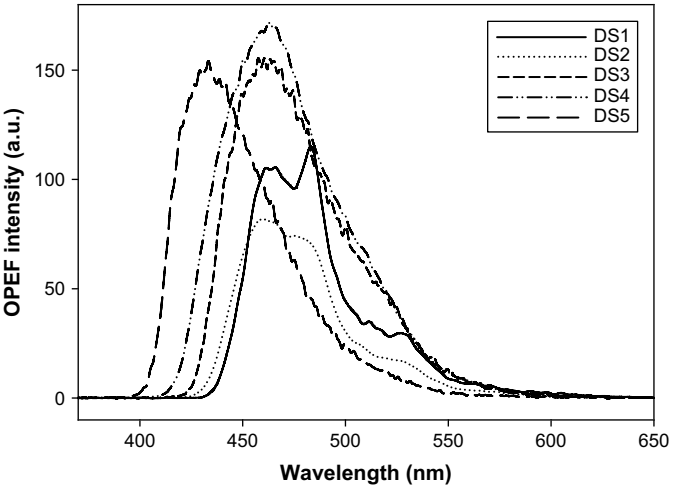

Fig. 5. The one-photon excited fluorescence spectra of the chromophores **DS1**–**DS5**.

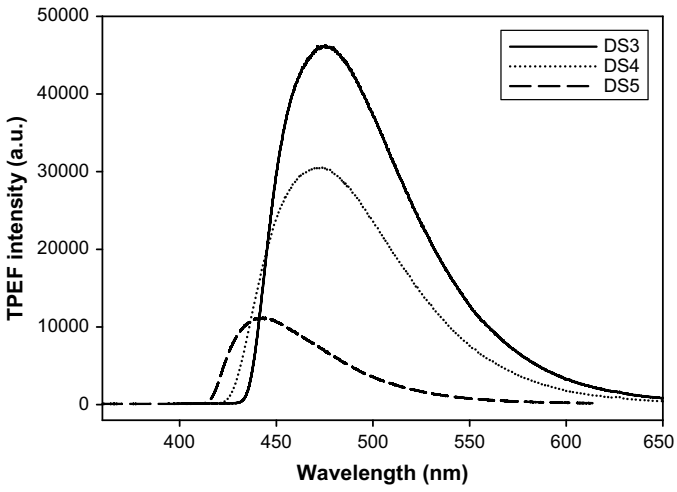

Fig. 6. The two-photon excited fluorescence spectra of the chromophores **DS3**–**DS5**.

planarity. In contrast, neither of 2,4,5-triarylimidazole or 3,5,6-triaryl-1,2,4-triazine units is planar [24,31,33]. For example, in 2,4,5-triphenyl imidazole derivatives [24,31], the planes of the three phenyl rings all twist out of the imidazole. Though these three phenyl rings could twist around the single bond between imidazole ring and three phenyl rings to a certain extent in solution, not all three phenyl rings can be turned to form a conjugated system with imidazole ring. Additionally, it has been reported that the benzoxazole ring system is essentially planar [23,34,35]. Therefore, among these compounds investigated here, the phenanthro[9,10-*d*]imidazole-benzoxazole hybrid **DS3** is more likely to possess a largest conjugated system and highly molecular planarity, and the peak position of **DS3** is red-shifted contrary to its counterparts.

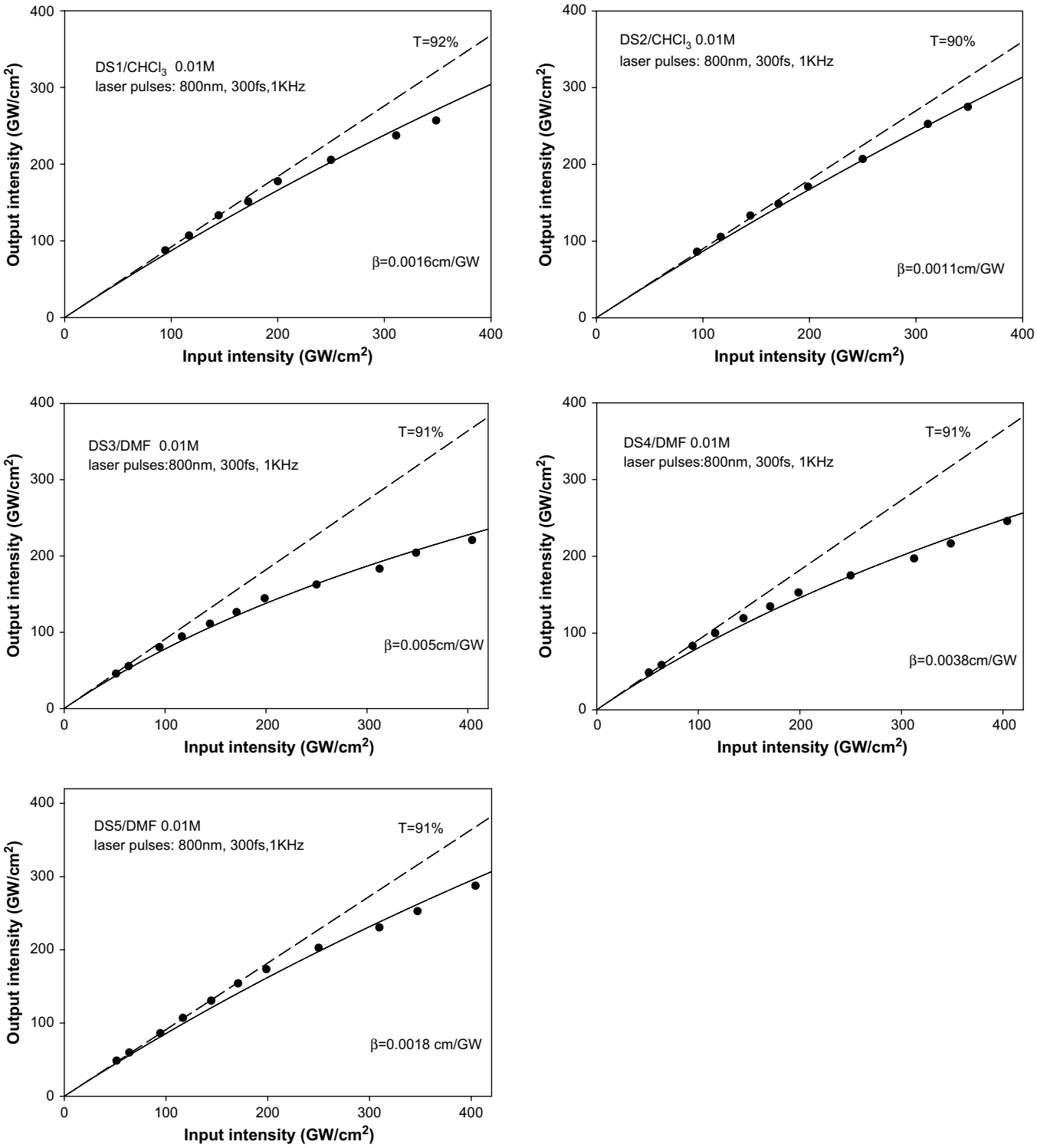

Fig. 7. Optical-limiting response of the chromophores **DS1**–**DS5**. The dashed lines correspond to the linear transmission of the solution, the scatter dots represent the experimental data and the solid lines are the theoretically fitted curve.

The one-photon excited fluorescence (**OPEF**) spectra for **DS1**, **DS2** in chloroform (3×10^{-5} mol L^{-1}) and **DS3**–**DS5** in DMF (1×10^{-5} mol L^{-1}) are shown in Fig. 5. Spectral parameters are shown in Table 2. From Fig. 5, one notices that three imidazole compounds (**DS3**–**DS5**) have similar fluorescence spectra, and none of these three fluorescence spectra have multiple peaks. While one strong emission peak near 461 nm is observed for **DS3** and **DS4**, the corresponding emission peak of **DS5** appears around 434 nm, which showed a hypsochromic shift of up to 27 nm with respect to that of **DS3** (461 nm). For compounds **DS1** and **DS2**, the emission maximum at 460, 480 nm and a shoulder at 530 nm were detected.

It is interesting to note that the Stokes shift values of the bis-1,2,4-triazine compounds **DS1** and **DS2** in chloroform solution, 15,528 and 14,624 cm^{-1}, respectively, are approximately four times of that of compound **DS5** in DMF (4206 cm^{-1}) (Table 2). It is considered that the differences in molecular conformation and charge distribution between molecular ground state and excited state of compounds **DS1** and **DS2** are more significant than those of other compounds.

3.4. Nonlinear photophysical properties

3.4.1. Two-photon excited fluorescence (TPEF)

The linear transmittance spectra of these five organic compounds in concentrated chloroform or DMF solution (1×10^{-2} mol L^{-1}) were also measured. No linear absorption in the wavelength range over 450 nm was observed, which implies that the emission induced by 800 nm excitation can be attributed to the nonlinear two-photon process.

When pumped with a laser pulse at 800 nm, all three compounds **DS3**–**DS5** at a concentration of 1×10^{-2} mol L^{-1} in DMF emit blue upconverted fluorescence (Fig. 6). The two-photon excited fluorescence of molecules **DS1** and **DS2** in chloroform solutions are too low to be detected. The profiles of the two-photon fluorescence spectra of compounds **DS3**–**DS5** are very similar to their corresponding one-photon fluorescence spectra, and their peak values are shown in Table 2. The emission maximum of the two-photon excited fluorescence for **DS3**, **DS4** and **DS5** are at ca. 476 nm, 474 nm and 443 nm, respectively.

By comparing Table 2, Fig. 5 and Fig. 6, we can see that the two-photon fluorescence maxima of compounds **DS3**–**DS5** have small red-shift (9–15 nm) compared with the corresponding one-photon fluorescence maxima in the same solvent. These red-shifts should be due to the re-absorption of the higher concentration solution (1×10^{-2} mol L^{-1}) used in TPEF compared to 1×10^{-5} mol L^{-1} used in OPEF.

3.4.2. TPA cross-section

TPA cross-section (σ_2) values of **DS1**, **DS2** in chloroform (1×10^{-2} mol L^{-1}) and **DS3**–**DS5** in DMF (1×10^{-2} mol L^{-1}) solutions were determined using nonlinear transmission (**NLT**) method with femtosecond laser pulses. The input–output power curves at 800 nm are presented in Fig. 7, where the dashed lines correspond to the linear transmission of the solution and the solid curves are fittings to the experimental results. With the best-fitting parameter of nonlinear absorption coefficient (β), the corresponding cross-sections (σ_2) are calculated based on the output power (I) as a function of incident intensity (I_0). The data for two-photon properties of molecules **DS1**–**DS5** obtained by nonlinear transmission method are listed in Table 2.

From Table 2, we noted that the TPA cross-sections of these molecules vary significantly, and have an order as **DS3** > **DS4** > **DS5** > **DS1** > **DS2**. Clearly, the σ_2 values of the two bis-1,2,4-triazine compounds are lower than those of all imidazole compounds, probably due to the poor molecular planarity and the weaker conjugation of these compounds. Furthermore, for compounds **DS1** and **DS2**, the structural modification just caused a slightly enhancement of TPA cross-section, owing to the relatively larger conjugation of 1,4-phenylene group.

On the other hand, we observe a strong enhancement of effective two-photon absorption for **DS3** that shows ~4.5 and ~2.8 times increase, relative to **DS2** and **DS5**, respectively. Compared with **DS4**, however, the σ_2 value of **DS3** was enhanced only ~5 GM.

From the viewpoint of molecular structure, **DS5** probably exhibits asymmetric intramolecular charge transfer and may decrease transition dipole moment, which will reduce molecular nonlinear absorption.

On the other hand, it is known that a planar geometry does not interfere with electron transfer across the molecule, and the less the electron transfer is impeded, the better the molecule should absorb and emit light. Therefore, the highest TPA cross-section ($\sigma_2 = 20.65$ GM) for molecule **DS3** can be ascribed to the extended π-delocalization system and its highly molecular planarity. Together, the electron acceptor pairs, imidazole and oxazole, attached to the π-center of the molecule, may increase the molecule dipole moment, and thereby lead to an increase in molecular optical nonlinearity.

As to molecule **DS4**, it could not possess a desired planar structure for phenyl ring planes and imidazole ring plane, though it has a very similar structure to **DS3**. This also explains why **DS4** has a higher σ_2 than **DS5**, but is lower than **DS3**.

These differences in the observed nonlinear absorption (effective TPA cross-section) are interesting because the structure modification in the phenanthro[9,10-*d*]imidazole moiety have a greater impact on the TPA properties than in the imidazole ring. It is evident that both phenanthro[9,10-*d*]imidazole and benzoxazole moieties are important for improving these desirable traits in a dye molecule, and the molecular planarity is the dominant factor for large two-photon cross-sections for the structures of **DS3** and **DS4**. Based on our results, it suggests that the phenanthro[9,10-*d*]imidazole-benzoxazole hybrids might become promising candidates as blue light-emitting TPA materials.

4. Conclusions

The synthesis, two-photon absorption and two-photon upconverted blue fluorescent emission properties for nitrogen-containing heterocycle chromophores are presented in this paper. The crystal structure of **DS6** was investigated by single crystal X-ray crystallography. It is found that the chromophores that possess the imidazole moiety exhibit strong two-photon upconverted blue emission peak at around 443–476 nm, and larger σ_2 values than those with the 1,2,4-triazine moiety. Therefore, imidazole derivatives were more potent two-photon absorption molecules than 1,2,4-triazine-based compounds. Experimental results indicate that significant enhancements in two-photon absorption cross-sections can be achieved by fusing of an benzoxazole moiety onto the phenanthro[9,10-*d*]imidazole ring. Such kind of structure modification is expected to be helpful in thoughtfully designing organic molecules with efficient two-photon induced blue emission for biological imaging.

5. Supplementary material

The crystallographic data (excluding structure factors) of **DS6** has been deposited with the Cambridge Crystallographic Center as supplementary publication no. CCDC 680351. Copy of this information may be obtained free of charge *via* www: http://www.ccdc.cam.ac.uk or from The Director, CCDC, 12 Union Road, Cambridge CB221EZ, UK (fax: +44 1223/336 033; email: deposite@ccdc.cam.ac.uk). Structural factors are available on request from the authors.

Acknowledgements

This project was supported by the National Natural Science Foundation of China (No. 10374013) and the Jiangsu Planned Projects for Postdoctoral Research Funds (No. 0701001B).

References

[1] Tian YP, Li L, Zhang JZ, Yang JX, Zhou HP, Wu JY, et al. Investigations and facile synthesis of a series of novel multi-functional two-photon absorption materials. J Mater Chem 2007;17:3646–54.
[2] Zhang M, Li MY, Zhao Q, Li FY, Zhang DQ, Zhang JP, et al. Novel Y-type two-photon active fluorophore: synthesis and application in fluorescent sensor for cysteine and homocysteine. Tetrahedron Lett 2007;48:2329–33.
[3] Xu GB, Hu DW, Zhao X, Shao ZS, Liu HJ, Tian YP. Fluorescence upconversion properties of a class of improved pyridinium dyes induced by two-photon absorption. Opt Laser Technol 2007;39:690–5.
[4] Mendonca CR, Neves UM, Boni LD, Andrade AA, Santos JDSD, Pavinatto FJ, et al. Two-photon induced anisotropy in PMMA film doped with Disperse Red 13. Opt Commun 2007;273:435–40.
[5] Huang ZZ, Wang XM, Li B, Lu CG, Xu J, Jiang WL, et al. Two-photon absorption of new multibranched chromophores based on bis(diphenylamino)stilbene. Opt Mater 2007;9:1084–90.
[6] Huang ZL, Li N, Lei H, Qiu ZR, Wang HZ, Zhong ZP, et al. Two-photon induced blue fluorescent emission of heterocycle-based organic molecule. Chem Commun 2002;20:2400–1.
[7] Zhao YX, Xiao L, Wu FP, Fang XY. Two-photon absorption properties of malononitrile derivatives. Opt Mater 2007;29:1206–10.
[8] Huang ZL, Li N, Sun YF, Wang HZ, Song HC, Xu ZL. Synthesis and structure–photophysical property relationships for two coumarinyl-based two-photon induced fluorescent molecules. J Mol Struct 2003;657:343–50.
[9] Liu B, Liu J, Wang HQ, Zhao YD, Huang ZL. Synthesis and spectroscopic properties of symmetrically substituted two-photon absorbing molecules with rigid elongated π-conjugation. J Mol Struct 2007;833:82–7.
[10] Gao B, Lu CG, Xu J, Meng FS, Cui YP, Tian H. Synthesis and two-photon properties of new perylene bisimide derivatives. Chem Lett 2006;35:1416–7.
[11] Xu F, Wang ZW, Gong QH. Synthesis, characterization, and optical properties of two-photon-absorbing octupolar molecule with an *s*-triazine core. Opt Mater 2007;29:723–7.
[12] Corredor CC, Huang ZL, Belfield KD. Two-photon 3D optical data storage via fluorescence modulation of an efficient fluorene dye by a photochromic diarylethene. Adv Mater 2006;18:2910–4.
[13] Kim HM, Fang XZ, Yang PR, Yi JS, Ko YG, Piao MJ, et al. Design of molecular two-photon probes for in vivo imaging. 2*H*-Benzo[*h*] chromene-2-one derivatives. Tetrahedron Lett 2007;48:2791–5.
[14] Li X, Zhao YX, Wang T, Shi MQ, Wu FP. Coumarin derivatives with enhanced two-photon absorption cross-sections. Dyes Pigments 2007;74:108–12.
[15] Sun YF, Cui YP. The synthesis, characterization and properties of coumarin-based chromophores containing a chalcone moiety. Dyes Pigments 2008;78:65–75.
[16] Sun YF, Song HC, Li WM, Xu ZL. Synthesis of 1,3,4-oxadiazole derivatives for organic electro-transporting electroluminescent materials. Chin J Org Chem 2003;23:1286–90.
[17] Bellina F, Cauteruccio S, Rossi R. Synthesis and biological activity of vicinal diaryl-substituted 1*H*-imidazoles. Tetrahedron 2007;63:4571–624.
[18] Hu ZJ, Yang JX, Tian YP, Zhou HP, Tao XT, Xu GB, et al. Synthesis and optical properties of two 2,2′:6′,2″-terpyridyl-based two-photon initiators. J Mol Struct 2007;839:50–7.
[19] Cui YZ, Fang Q, Huang ZL, Xue G, Yu WT, Lei H. Synthesis, structure, and intense second harmonic generation of K-shaped *s*-triazine derivative. Opt Mater 2005;27:1571–5.
[20] Tsai MH, Hong YH, Chang CH, Su HC, Wu CC, Matoliukstyte A, et al. 3-(9-Carbazolyl) carbazoles and 3,6-di(9-carbazolyl)carbazoles as effective host materials for efficient blue organic electrophosphorescence. Adv Mater 2007;19:862–6.
[21] Fridman N, Kaftory M, Speiser S. Structures and photophysics of lophine and double lophine derivatives. Sens Actuators B 2007;126:107–15.
[22] Mac M, Tokarczyk B, Uchacz T, Danel A. Charge transfer fluorescence of benzoxazol derivatives. Investigation of solvent effect on fluorescence of these dyes. J Photochem Photobiol A Chem 2007;191:32–41.
[23] Karolak-Wojciechowska J, Mrozek A, Czylkowski R, Tekiner-Gulbas B, Akı-Sener E, Yalcin I. Five-membered heterocycles. Part IV: Impact of heteroatom on benzazole aromaticity. J Mol Struct 2007;839:125–31.
[24] Pan WL, Tan HB, Chen Y, Mu DH, Liu HB, Wan YQ, et al. The synthesis and preliminary optical study of 1-alkyl-2,4,5-triphenylimidazole derivatives. Dyes Pigments 2008;76:17–23.
[25] Um SI. The synthesis and properties of benzoxazole fluorescent brighteners for application to polyester fibers. Dyes Pigments 2007;75:185–8.
[26] Hudson MJ, Foreman MRSJ, Hill C, Huet N, Madic C. Studies on the parallel synthesis and evaluation of new heterocyclic extractants for the partitioning of minor actinides. Solvent Extr Ion Exch 2003;21:637–52.
[27] Sun YF, Pan WL, Wu RT, Song HC. Microwave-assisted synthesis and fluorescence characterization of bis-1,2,4-triazine derivatives. Chin J Org Chem 2006;8:1079–82.
[28] He GS, Xu GC, Prasad PN, Reinhardt BA, Bhatt JC, Dillard AG. Two-photon absorption and optical-limiting properties of novel organic compounds. Opt Lett 1995;20:435–7.
[29] Morita K, Suehiro T, Yokoh Y, Ashitaka H. The development of organic third-order nonlinear optical materials. J Photopolym Sci Technol 1993;6:229–38.
[30] Li HW, Zhu WX. Crystal structure of adduct 2-phenyl-imidazo[4,5-*f*]1,10-phenanthroline methanol. Chin J Chem 2003;21:1054–8.
[31] Liu XF, Zhong ZP, Xu ZL. 4-[4,5-Bis(4-methoxyphenyl)-1*H*-imidazol-2-yl] benzonitrile. Acta Crystallogr 2005;E61:o1976–7.
[32] Sun YF, Cui YP, Li JK, Zheng ZB. 2-(4-Hydroxy-3,5-dimethoxy phenyl)-1*H*-phenanthro[9,10-*d*]imidazole methanol solvate. Acta Crystallogr 2007;E63:o1751–2.
[33] Eltayeb NE, Teoh SG, Ng SL, Fun HK, Ibrahim K. 5,6-Diphenyl-3-(2-pyridyl)-1,2,4-triazine. Acta Crystallogr 2007;E63:o1041–2.
[34] Vinsorva J, Marek J, Vanco J, Csollei J. 5,7-Di-tert-butyl-2-(2-pyridyl) benzo[*d*]oxazole. Acta Crystallogr 2007;E63:o2802–3.
[35] Franca EF, Machado AEH, Oliveira-Campos AMF, Santos S, Ellena J, Guilar S. 3-(Benzoxazol-2-yl)-7-hydroxychromen-2-one methanol solvate. Acta Crystallogr 2003;E59:o820–2.